



Dynamic positioning, system identification and control of marine vessels

Nour Bargouth¹ Christer Dalen² David Di Ruscio³

¹University of South-Eastern Norway, P.O. Box 203, N-3901 Porsgrunn, Norway. E-mail: 238957@usn.no

²Skien, Norway. E-mail: christerdalen@hotmail.com

³University of South-Eastern Norway, P.O. Box 203, N-3901 Porsgrunn, Norway. E-mail: David.Di.Ruscio@usn.no

Abstract

In this paper, various modern model based optimal control methods (as well as one model-free or data-driven) are applied to the dynamical positioning problem of vessels, i.e. we seek to control the surge, sway and yaw motion, using the thrusters and propellers, subject to environmental disturbances, i.e. wind and current. The low-frequency part of Balchen's nonlinear vessel model is selected for these tests.

Keywords: Dynamic positioning, Kalman filtering, optimal control, model free, linear quadratic, model predictive, control

1. Introduction

The dynamic positioning of marine vessels is an important issue especially in the oil and gas industry for safety and economic demands. A great amount of research had been done to develop efficient dynamic positioning systems but one of the challenges was about finding an accurate mathematical model to be used in developing model based control systems.

A DP system based on modern model control theory was first proposed and implemented in the work of Balchen et al. (1980). See also the works of Saelid et al. (1983); Sørensen et al. (1996).

We are using the low frequent part of the nonlinear Balchen et al. (1980) model in order to test different optimal control methods for Dynamic Positioning (DP) of marine vessels. A DP system, generally, includes a position and heading measurement system, a controller algorithm, and a propulsion system. In this paper, we focus on the controller algorithms of the DP system. A DP system may be defined as a computer system which automatically controls the position as well as the heading, of a vessel, by using its propellers and thrusters.

With optimal control, methods we are including Model Predictive Control (MPC) methods and a total of five MPC and optimal control methods are tested.

In this paper, standard MPC, MPC with integral action Di Ruscio (2013), and optimal control with integral action Di Ruscio (2012) are implemented and tested to control the position and rotation/heading of a selected vessel. See Figure 1 for illustration.

The contributions in this paper may be itemized as follows:

- MPC Di Ruscio (2013), Linear Quadratic (LQ) Di Ruscio (2012), Model based, and model free control methods (Dalen et al. (2015)) are applied to the nonlinear Balchen model in Balchen et al. (1980).

All numerical calculations and plotting facilities are provided by using the MATLAB software (MATLAB (2020)).

The rest of this paper is organized as in the following. In Section 2 the nonlinear model is presented. In Section 3 the optimal control theory is given. In Section 4 the numerical examples are given. In Section 5

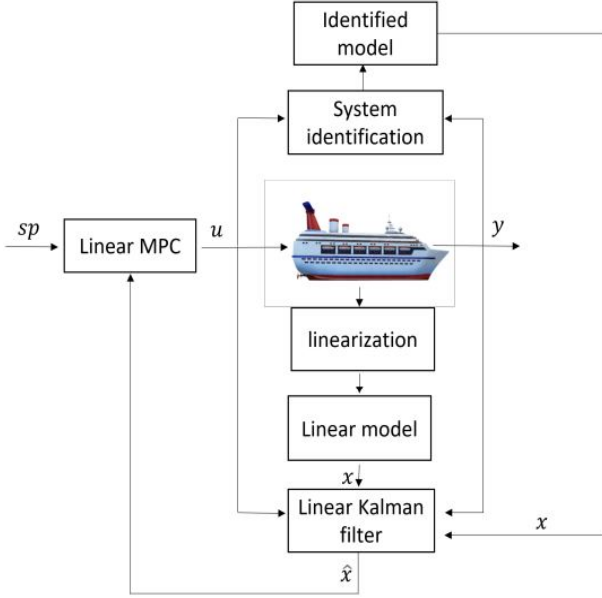


Figure 1: The figure is illustrating the Dynamic Positioning control system with linear MPC, linear model and identified model. By 'linearization'-block it is assumed that a model is available describing the vessel dynamics.

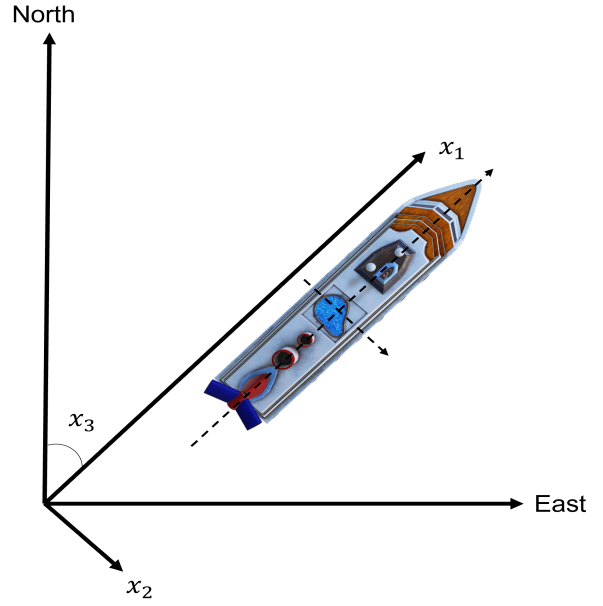


Figure 3: The figure is illustrating the NED and Body coordinate systems.

the concluding and discussion remarks are given.

2. Nonlinear Vessel Model

In the following, a nonlinear continuous state space model describing a marine vessel is described, viz. this is the low frequent part of the model presented in [Balchen et al. \(1980\)](#).

Consider,

$$\dot{x} = f(x, u), \quad (1)$$

$$y = g(x), \quad (2)$$

where

$$y \in \mathbb{R}^3 := \begin{cases} y_1: \text{Position Surge, [m]} \\ y_2: \text{Position Sway, [m]} \\ y_3: \text{Heading Yaw, [rad]} \end{cases} \quad (3)$$

$$u \in \mathbb{R}^3 := \begin{cases} u_1: \text{Control Surge, [N]} \\ u_2: \text{Control Sway, [N]} \\ u_3: \text{Control Yaw, [Nm]} \end{cases} \quad (4)$$

$$x \in \mathbb{R}^6 := \begin{cases} x_1: \text{Position Surge, [m]} \\ x_2: \text{Position Sway, [m]} \\ x_3: \text{Position Yaw, [rad]} \\ x_4: \text{Velocity Surge, [m/s]} \\ x_5: \text{Velocity Sway, [m/s]} \\ x_6: \text{Velocity Yaw, [rad/s]} \end{cases} \quad (5)$$

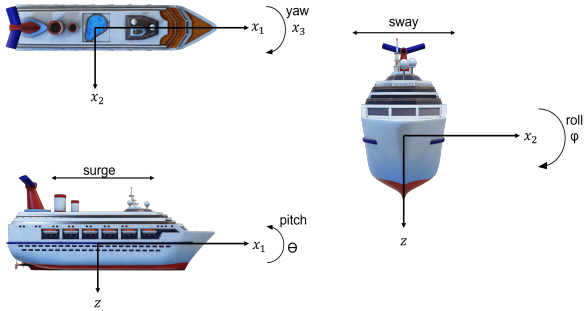


Figure 2: The figure is illustrating the 3 degrees of freedom of a vessel. For DP systems we are interested in controlling 3 degrees of freedom, surge, sway and yaw. The figure illustrates motion and rotation variables for a Vessel.

$$\dot{x}_1 = x_4, \quad (6)$$

$$\dot{x}_2 = x_5, \quad (7)$$

$$\dot{x}_3 = x_6, \quad (8)$$

$$\begin{aligned} \dot{x}_4 &= -\frac{d_1}{m_1}|x_4 - \nu_{c_{su}}|(x_4 - \nu_{c_{su}}) \\ &+ \frac{1}{m_1}(F_{w_{su}} + u_1), \end{aligned} \quad (9)$$

$$\begin{aligned} \dot{x}_5 &= -\frac{d_2}{m_2}|x_5 - \nu_{c_{sw}}|(x_5 - \nu_{c_{sw}}) \\ &+ \frac{1}{m_2}(F_{w_{sw}} + u_2), \end{aligned} \quad (10)$$

$$\begin{aligned} \dot{x}_6 &= -\frac{d_3}{m_3}|x_6| x_6 - \frac{d_4}{m_3}|x_5 - \nu_{c_{sw}}|(x_5 - \nu_{c_{sw}}) \\ &+ \frac{1}{m_3}(N_w + u_3 + N_c), \end{aligned} \quad (11)$$

where m_1 , m_2 and m_3 are the inertial coefficients which are assumed to be constants. d_1 , d_2 , d_3 and d_4 are the drag and moment coefficients.

See Figures 2 and 3 for the body coordinate and illustration of the states described in Eq. (5).

2.1. Forces and Moments

Environmental forces and moments have to be transformed from the NED to Body coordinate system to calculate vessel position and velocity.

We have that,

$$V_c = R^T V_c^{NED}, \quad (12)$$

where

$$V_c \in \mathbb{R}^3 := \begin{cases} \nu_{c_{su}}: \text{water current velocity Surge [m/s]} \\ \nu_{c_{sw}}: \text{water current velocity Sway [m/s]} \\ N_c: \text{water current moment Yaw [Nm]}, \end{cases} \quad (13)$$

V_c^{NED} : water current velocity components in the NED coordinate system, and

$$R = \begin{bmatrix} \cos(x_3) & -\sin(x_3) & 0 \\ \sin(x_3) & \cos(x_3) & 0 \\ 0 & 0 & 1 \end{bmatrix}, \quad (14)$$

is the transformation matrix.

Wind forces in surge and sway and wind effect in yaw are proportional to wind density ρ , wind relative speed V_r , wind angle of attack γ and windage area, viz.

$$F_w = \frac{1}{2}\rho V_r^2 \begin{bmatrix} C_x \cos(\gamma) A_F \\ C_y \sin(\gamma) A_L \\ C_N \sin(2\gamma) A_L L \end{bmatrix}, \quad (15)$$

where

$$F_w \in \mathbb{R}^3 := \begin{cases} F_{w_{su}}: \text{wind force Surge [N]} \\ F_{w_{sw}}: \text{wind force Sway [N]} \\ N_w: \text{wind moment Yaw [Nm]}, \end{cases} \quad (16)$$

and

$$u_w = V_w \cos(\beta - x_3), \quad (17)$$

$$v_w = V_w \sin(\beta - x_3), \quad (18)$$

$$u_{rw} = x_4 - u_w, \quad (19)$$

$$v_{rw} = x_5 - v_w, \quad (20)$$

$$V_r = \sqrt{u_{rw}^2 + v_{rw}^2}, \quad (21)$$

where β is the measured wind direction, V_w is the measured wind speed, C_x , C_y , C_N are the wind coefficients (assumed constant), A_L , A_F windage area for beam wind and headwind i.o. and L is the vessel overall length.

3. Optimal Control Methods

3.1. System Definition

We will restrict ourselves to linearized or linear state space dynamic models of the form

$$x_{k+1} = Ax_k + Bu_k + v, \quad (22)$$

$$y_k = Dx_k + w, \quad (23)$$

where $x_k \in R^n$ is the state vector, $u_k \in R^r$ is the control input vector, $y_k \in R^m$ is the output (measurement) vector, A , B and D are system matrices of appropriate dimensions, and x_0 is the initial state. The disturbances v and w may both be unknown, i.e., v may be an unknown constant or slowly varying process disturbance, and w may be an unknown constant or slowly varying measurements noise vector. v and w may represent trends or drifts.

Most of the optimal control methods evolve around minimizing the following LQ cost function, performance index,

$$J_k = (y_{k+1|L} - r_{k+1|L})^T Q (y_{k+1|L} - r_{k+1|L}) + \Delta u_{k|L}^T P \Delta u_{k|L}, \quad (24)$$

where $Q \in R^{LmLm}$ is a block diagonal matrix with $Q_i \forall i = 1, \dots, L$ on the block diagonal. $P \in R^{LrLr}$

is defined similar with $P_i \forall i = 1, \dots, L$ on the block diagonal. The notation used to define the vectors in Eq. (4) is defined in Appendix A in Di Ruscio (2013).

In this paper, we consider the input rate of change and amplitude constraints. These constraints may be formulated as a linear inequality

$$\mathcal{A}\Delta u_{k|L} \leq b_k, \quad (25)$$

where the expressions for \mathcal{A} and b_k may be found in Section 3.2 in Di Ruscio (2013). Where b_k is an unknown vector of future control increments, subject to the process constraints,

$$\Delta u_{k|L}^* = \arg \min_{\mathcal{A}\Delta u_{k|L} \leq b_k} J_L. \quad (26)$$

In this paper, we use the following Kalman filter/State observer, Di Ruscio (2012),

$$\bar{x}_{k+1} = A\bar{x}_k + Bu_k + K(y_k - D\bar{x}_k), \quad (27)$$

where \bar{x}_0 is the initial estimate.

The optimal control methods used in this paper are briefly described and defined in the following. For detailed descriptions look up the corresponding references.

- Nonlinear MPC (**mpc**). See Morari et al. (1988).
- Nonlinear MPC reduced variant (**mpc_red**). See Morari et al. (1988).
- MPC with integral action (**mpc_int**) is defined in the paper of Di Ruscio (2013).
- LQ with integral action (**lq_int**) is defined as the method presented in the paper of Di Ruscio (2012).
- Model free LQ control (**mflqc**) is presented in the work of Dalen et al. (2015).

The underlying goal of this paper is to test and compare the previous enumerated list, i.e. these five DP system control algorithms.

4. Numerical Examples

In the incoming example, we will compare the DP system **mpc**, **mpc_red**, **mpc_int**, **lq_int** and **mflqc** controller algorithms on the nonlinear Balchen marine vessel model described in Section 2. The nonlinear Balchen model m-file function is available in the appendix A.

We adopt the performance indices from Åström and Hägglund (1995); Seborg et al. (1989); Skogestad (2003). In order to measure performance in a feedback

system (See Figure 1), the Integrated Absolute Error (IAE) is defined as,

$$IAE = \int_0^\infty |e(t)| dt, \quad (28)$$

where, r , is the reference/setpoint and, $e = r - y$, is the error.

To evaluate the amount of input usage we include the following Total input Value (TV) measure,

$$TV = \int_0^\infty |\Delta u_k| dt, \quad (29)$$

where, $\Delta u_k = u_k - u_{k-1}$, is the control rate of change.

For surge-sway reference/setpoint responses, we introduce a combined IAE, i.e.

$$\sum IAE = IAE_{surge} + IAE_{sway}, \quad (30)$$

$$\sum TV = TV_{surge} + TV_{sway}. \quad (31)$$

The Figures 4, 5 and 6 show the reference/setpoint step response for the five DP system **mpc**, **mpc_red**, **mpc_int**, **lq_int** and **mflqc** controller algorithms, viz. surge is set from 0 to 3 m, sway position is set from 0 to 5 m, and yaw rotation/heading set from 0 to 3 m at time equal 200 samples for the algorithms. In Figure 7 the corresponding position is shown in NED frame.

In the surge-sway position, the **mpc_int** algorithm is seen to have an edge over the other algorithms, viz. in Table 3 (rows 2:6, column 2), the **mpc_int** algorithm is seen to be, $\frac{\sum IAE_{mpc}}{\sum IAE_{mpc_int}} = 4.8174$, $\frac{\sum IAE_{mpc_red}}{\sum IAE_{mpc_int}} = 6.3583$, $\frac{\sum IAE_{lq_int}}{\sum IAE_{mpc_int}} = 2.9072$, and $\frac{\sum IAE_{mflqr}}{\sum IAE_{mpc_int}} = 2.5743$, times better than **mpc**, **mpc_red**, **lq_int** and **mflqc**, i.o., in terms of the performance index, combined $\sum IAE$ (Eq. (30)).

Furthermore, in the yaw rotation/heading, the **mpc_int** algorithm is seen to have an edge over the other algorithms, viz. in Table 3 (rows 2:6, column 2), the **mpc_int** algorithm is seen to be, $\frac{IAE_{mpc}}{IAE_{mpc_int}} = 12.4352$, $\frac{IAE_{mpc_red}}{IAE_{mpc_int}} = 14.4856$, $\frac{IAE_{lq_int}}{IAE_{mpc_int}} = 7.8270$, and $\frac{IAE_{mflqr}}{IAE_{mpc_int}} = 7.9020$, times better than **mpc**, **mpc_red**, **lq_int** and **mflqc**, i.o., in terms of the performance index, IAE (Eq. (28)).

In the surge-sway position, the **mpc** algorithm is seen to have outperformance over the other algorithms, viz. in Table 2 (rows 2:6, column 3), the **mpc** algorithm is seen to be, $\frac{\sum TV_{mpc_red}}{\sum TV_{mpc}} = 3.1822$, $\frac{\sum TV_{mpc_int}}{\sum TV_{mpc}} = 2.5141$, $\frac{\sum TV_{lq_int}}{\sum TV_{mpc}} = 1.7268$, and $\frac{\sum TV_{mflqr}}{\sum TV_{mpc}} = 2.4860$, times better than **mpc_red**,

mpc_int, **lq_int** and **mflqr**, i.o., in terms of the input usage, $\sum TV$ (Eq. (31)).

Furthermore, in the yaw rotation/heading, the **mpc_red** algorithm is seen to have an edge over the other algorithms, viz. in Table 2 (rows 2:6, column 3), the **mpc_red** algorithm is seen to be, $\frac{TV_{mpc}}{TV_{mpc_red}} = 1.0967$, $\frac{TV_{mpc_int}}{TV_{mpc_red}} = 149.8967$, $\frac{TV_{lq_int}}{TV_{mpc_red}} = 8.7734$, and $\frac{TV_{mflqr}}{TV_{mpc_red}} = 7.7186$, times better than **mpc**, **mpc_int**, **lq_int** and **mflqr**, i.o., in terms of the performance index, TV (Eq. (29)).

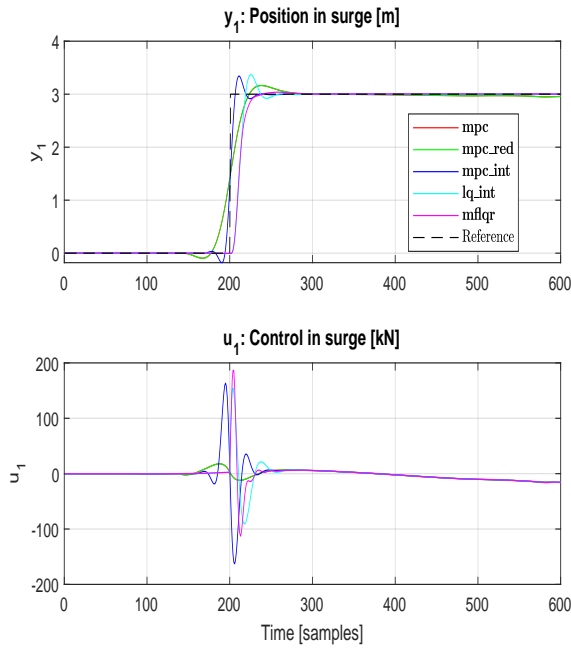


Figure 4: The figure shows the reference/setpoint step in surge position for the five different DP systems controller algorithms.

Table 1: The table shows the combined (surge-sway) mean Integral Absolute Error indices $\sum IAE$ (Eq. (30)) and mean Total input Value (Eq. (31)) for **mpc**, **mpc_red**, **mpc_int**, **lq_int** and **mflqr** algorithms corresponding to reference/setpoint response in surge and sway.

Algorithm	$\sum IAE$	$\sum TV$
mpc	86.12	2752.81
mpc_red	113.67	8760.05
mpc_int	17.88	6920.71
lq_int	51.97	4753.42
mflqr	46.02	6843.41

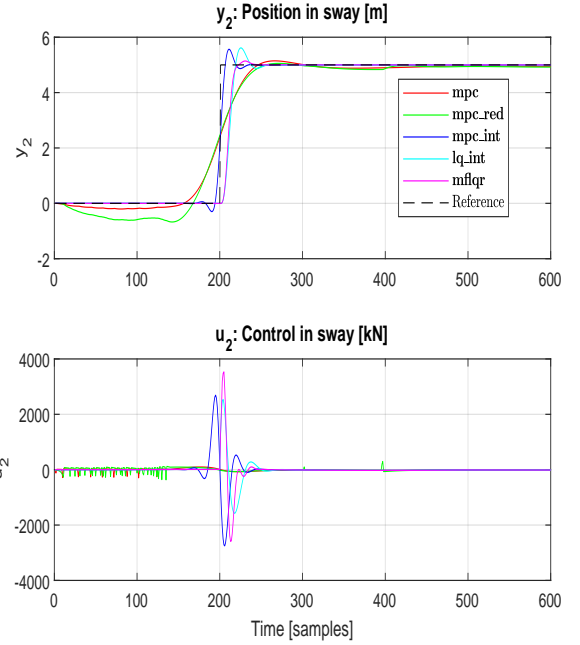


Figure 5: The figure shows the reference/setpoint step in sway position for the five different DP systems controller algorithms.

Table 2: The table shows the Integral Absolute Error indices IAE (Eq. (28)) and Total input Value (Eq. (29)) for **mpc**, **mpc_red**, **mpc_int**, **lq_int** and **mflqr** algorithms corresponding to reference/setpoint response in yaw rotation/heading.

Algorithm	IAE	TV
mpc	119.69	3369.26
mpc_red	139.42	3072.14
mpc_int	9.62	460503.95
lq_int	75.34	26953.16
mflqr	76.06	23712.71

Table 3: The table shows the mean execution time for **mpc**, **mpc_red**, **mpc_int**, **lq_int** and **mflqr** algorithms for each time step. Mean @ Standard Deviation.

Algorithm	Execution Time
mpc	0.1655 @ 0.0195
mpc_red	0.0559 @ 0.0180
mpc_int	0.0337 @ 0.0112
lq_int	2.99e-06 @ 2.51e-05
mflqr	3.47e-06 @ 2.78e-05

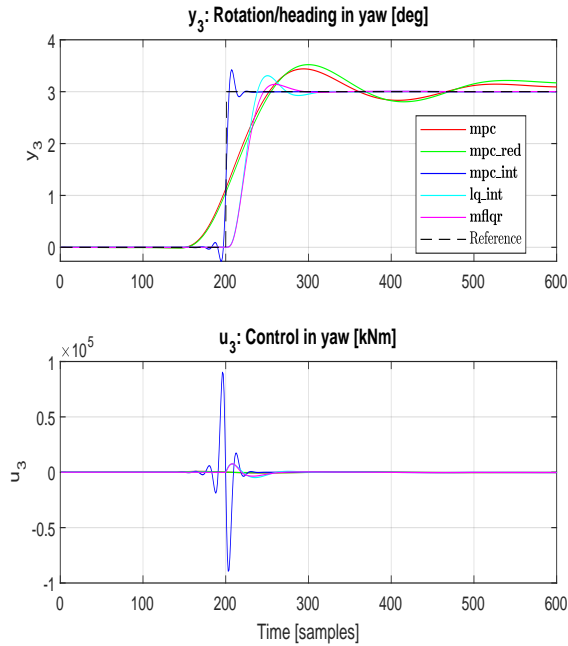


Figure 6: The figure shows the reference/setpoint step in yaw rotation/heading for the five different DP systems controller algorithms.

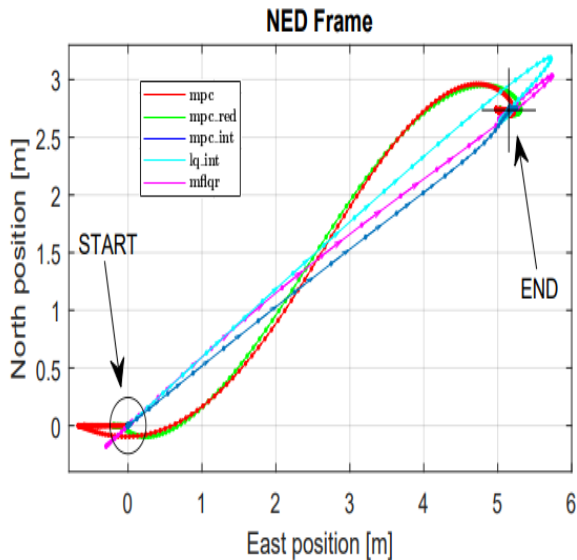


Figure 7: NED and Body coordinate systems.

5. Concluding and Discussion Remarks

Five different DP system controller algorithms were tested and compared on a nonlinear Balchen vessel model. Concluding Remarks on the results from the numerical example in Section 4.

- The DP system **mpc_int** controller algorithm is shown to have an edge over the other DP system controller algorithms in terms of reference/setpoint step response, viz. in surge-sway position and yaw rotation/heading, the **mpc_int** algorithm is seen to be atleast, $\frac{\sum IAE_{mflqr}}{\sum IAE_{mpc.int}} = 2.5743$, and, $\frac{IAE_{lq.int}}{IAE_{mpc.int}} = 7.8270$, times better, i.o., than the other algorithms.
- The DP system **mpc** controller algorithm is shown to have an edge over the other DP system controller algorithms in terms of input usage, viz. in surge-sway position the **mpc** algorithm is seen to be atleast, $\frac{\sum TV_{lq.int}}{\sum TV_{mpc}} = 1.7268$, times better than the other algorithms. In yaw rotation/heading, the **mpc.red** algorithm is seen atleast $\frac{TV_{mpc}}{TV_{mpc.red}} = 1.0967$, times better than the other algorithms.
- The **mpc** and **mpc.red** algorithms are seen relatively slow at reference/setpoint tracking. One may argue that by changing weights could solve this, however making it faster could probably enhance the undesirable "spikes" seen in Figure 4 for **mpc** and **mpc.red**.
- The execution time of **mflqr** and **lq.int** is seen similar and atleast 9712 times faster than the other three algorithms. See Table 3.
- In terms of yaw rotation/heading, the DP system **mpc_int** controller has a large control input, almost $1e5$ kNm, (see subplot row 2, column 1 in Figure 6) and TV, (see row 4, column 3 in Table 2). This large control input compared to the other methods probably explains the outperformance of **mpc_int**. These values may seem unrealistic in a practical case. This large control input u_3 may be reduced by adjusting the corresponding weight in the **mpc_int** algorithm.

A. Nonlinear model

Balchen nonlinear (Balchen et al. (1980)) vessel m-file implementation

```

function f = balchen_vess(x,u,F_w,F_c)

m1 = 4 * 10^6;
m2 = 4 * 10^7;
m3 = 4.7 * 10^10;
d1 = 5*10^-5;
d2 = 21*10^-5;
d3 = 1.1*10^-10;
d4 = 201*10^-15;

f=zeros(6,1);
f(1) = x(4);
f(2) = x(5);
f(3) = x(6);
f(4) = - d1/m1*abs(x(4) - F_c(1))*(x(4) ...
- F_c(1)) + 1/m1*(F_w(1) + F_t(1));
f(5) = - d2/m2*abs(x(5) - F_c(2))*(x(5) ...
- F_c(2)) + 1/m2*(F_w(2) + F_t(2));
f(6) = - d3/m3*abs(x(6))*x(6)...
- d4/m3*abs(x(5) - F_c(2))*(x(5) - F_c(2))...
+ 1/m3*(F_w(3) + F_t(3) + F_c(3));

end

```

References

- Åström, K. and Hägglund, T. *PID Controllers: Theory, Design, and Tuning*. Instrument Society of America, 1995.
- Balchen, J. G., Jenssen, N. A., Mathisen, E., and Slid, S. A Dynamic Positioning System Based on Kalman Filtering and Optimal Control. *Modeling, Identification and Control*, 1980. 1(3):135–163. doi:[10.4173/mic.1980.3.1](https://doi.org/10.4173/mic.1980.3.1).
- Dalen, C., Di Ruscio, D., and Nilsen, R. Model-free optimal anti-slug control of a well-pipeline-riser in the K-Spice/LedaFlow simulator. *Modeling, Identification and Control*, 2015. 36(3):179–188. doi:[10.4173/mic.2015.3.5](https://doi.org/10.4173/mic.2015.3.5).
- Di Ruscio, D. Discrete LQ optimal control with integral action: A simple controller on incremental form for MIMO systems. *Modeling, Identification and Control*, 2012. 33(2):35–44. doi:[10.4173/mic.2012.2.1](https://doi.org/10.4173/mic.2012.2.1).
- Di Ruscio, D. Model Predictive Control with Integral Action: A simple MPC algorithm. *Modeling, Identification and Control*, 2013. 34(3):119–129. doi:[10.4173/mic.2013.3.2](https://doi.org/10.4173/mic.2013.3.2).
- MATLAB. *version 9.9.0.1718557 (R2020b)*. The MathWorks Inc., Natick, Massachusetts, USA, 2020. Control System Toolbox, Version 10.9. System Identification Toolbox, Version 9.13.
- Morari, M., Garcia, C. E., and Pretti, D. M. Model predictive control: Theory and practice. *IFAC Proceedings Volumes*, 1988. 21(4):1–12. doi:<https://doi.org/10.1016/B978-0-08-035735-5.50006-1>. IFAC Workshop on Model Based Process Control, Atlanta, GA, USA, 13-14 June.
- Saelid, S., JENSSEN, N., and BALCHEN, J. Design and analysis of a dynamic positioning system based on kalman filtering and optimal control. *Automatic Control, IEEE Transactions on*, 1983. 28:331 – 339. doi:[10.1109/TAC.1983.1103225](https://doi.org/10.1109/TAC.1983.1103225).
- Seborg, D., Edgar, T. F., and Mellichamp, D. A. *Process Dynamics and Control*. John Wiley and Sons, 1989.
- Skogestad, S. Simple analytic rules for model reduction and PID controller tuning. *Journal of Process Control*, 2003. 13(4):291–309. doi:[10.1016/S0959-1524\(02\)00062-8](https://doi.org/10.1016/S0959-1524(02)00062-8).
- Sørensen, A. J., Sagatun, S. I., and Fossen, T. I. Design of a dynamic positioning system using model-based control. *Modeling, Identification and Control*, 1996. 17(2):135–151. doi:[10.4173/mic.1996.2.6](https://doi.org/10.4173/mic.1996.2.6).